THE AMERICAN SOCIETY OF MECHANICAL ENGINEERS
345 E. 47th St., New York, N.Y. 10017

97-GT-97

ENTROPY GENERATION IN A 2-D CASCADE AT DIFFERENT ANGLES OF ATTACK: A NUMERICAL STUDY

Gianni NATALINI, Enrico SCIUBBA

Dipartimento di Meccanica ed Aeronautica,
Universita' di Roma 1 - "La Sapienza"

ABSTRACT

This paper presents the results of an entropy generation calculation made on a representative gas turbine rotor blade; in particular, the numerical study has dealt with the different flowfields which are encountered when the angle of attack is varied in a two-dimensional cascade on axial, internally cooled gas turbine rotor.

The analysis takes into consideration a two-dimensional cascade at medium Reynolds number (Re_{chord}=225000), sub-sonic Mach number (Ma_{in}=0.27), and steady state. The full Navier-Stokes equations of motion for a turbulent compressible viscous flow, together with the appropriate energy equation, are solved via a standard finite elements code with a k-ε closure, so that complete velocity- and temperature fields are obtained (including boundary-layer effects, via proper wall functions). These fields are then used to compute the entropy generation rates corresponding to the viscous- ($\dot{S}_v$) and thermal ($\dot{S}_t$) dissipation.

Several configurations have been numerically tested, the reference one being at design conditions, and the remaining being obtained from it by varying the angle of attack α (defined as the angle, measured ccw, between the relative velocity vector W_1 and the tangent to the blade chord at impingement point), to simulate volume flowrate variations.

A commercial finite-element code (FIDAP, by FDI Inc.) has been modified to allow for the calculation of the *local* values of the entropy generation rates, the thermal- and viscous portions of which have been computed separately.

The results at design point are shown to agree well with the available cascade performance data.

The entropy generations rates are then used to compute the so-called entropy loss coefficient (a better name for which would be that of *irreversibility coefficient*, ζ, defined as:

$$\zeta = \frac{T_0 \Delta s}{h_{1s} - h_{2i}}$$

where T_0 is the reference ambient temperature, Δs is the *total local* entropy generation rate (sum of the viscous- and thermal components), and h_{1s} and h_{2i} are the stagnation enthalpy upstream of the rotor and the ideal exit enthalpy respectively.

The results are shown under the form of c_p - and ζ graphs computed for different angles of attack α (from -4.4 to +7.6 degrees), and are representative of realistic situations which could arise in actual gas turbine rotors. The loss coefficient ζ is shown to attain a minimum value at design point.

Integral values for the entropy generation rates are also computed, and *total entropy losses* are thus computed for the various configurations. Maps of the viscous- and thermal entropy generation rates are shown for each angle of attack, where of interest.

Presented at the International Gas Turbine & Aeroengine Congress & Exhibition
Orlando, Florida — June 2–June 5, 1997

1- INTRODUCTION

Energy conversion plants based on gas turbines, either in stand-alone or in combined-cycle installations, are not only an established power-producing technology, but also a very active field of both theoretical and applied research: the very structure of these plants, in fact, poses very high demands on materials and confronts the designer with fundamental -and quite difficult-fluid- and thermodynamic problems.

In the years, enormous technological efforts have therefore been devoted to the improvement of the performance of components of gas turbine plants, and the result has been a remarkable increase of their overall conversion efficiency, from the roughly 25% of the 1960 models to the over 37% of some 1994 models.

To improve *cycle* efficiency so drastically, both pressure ratio and combustion temperature have to be increased, and they are of course functionally linked to each other, so that a given turbine entry temperature requires a certain well-defined "optimal" pressure ratio. The increase in turbine entry temperature has been slowed down by the thermo-mechanical limitations posed by the necessity of reducing the level of thermal stresses in the first stage bladings; however, it is not uncommon today to observe 25:1 pressure ratios together with an 1800 K gas turbine temperature at turbine inlet, at least in advanced, high-performance jet engines. Furthermore, even heavy-duty gas turbines have inlet temperatures well above 1400 K.

For such temperatures, efficient blade cooling is mandatory: first-row nozzles and blades (and sometimes, second-row nozzles) are usually cooled by routing compressor air (dry or in some instances humidified by water or steam injection) into the vane root, and letting it expand along radial holes internal to the vane (fig. 1), before being discharged into the main stream through a series of "slots" or "holes" properly placed on the vane external surface.

The effectiveness of film cooling on the stator vanes depends on nozzle geometry and location and number of the cooling holes; on the rotating blade, rotation and unsteadiness effects come also into play. To correctly design a cooled vane, and to choose the most appropriate configuration, it is very important to fully understand the flow characteristics in the entire stage (nozzle + rotor). Flow- and thermal losses can be properly measured by the irreversible entropy production associated with each one of them: recently, the calculation of entropy generation has been shown to be the only *rational* measure of flow losses [6,13,14], and the results of several routine calculations of interest for gas turbine components have been published [2,3,4,6,8,9,11].

Irreversible losses in gas turbine engines are originated by:

- mechanical friction in bearings, seals, gearboxes, auxiliary power outlets, etc.;

- viscous dissipation in the fluid, which causes pressure losses both in the main and in the cooling circuit;

- thermal non-uniformities, both in the fluid and in the rotor/casing material, which originate irreversible temperature gradients in the interaction of the fluid with the machine.

Then, an appropriate approach to the design problem could be that of *minimizing the overall amount of irreversible losses, for a certain machine configuration, and for given values of blade loading and of maximum allowable thermal stress.*

These losses ought to be taken into account *qualitatively* as well as *quantitatively*, and this can be done by calculating the entropy generation rate separately produced by each loss: then it becomes possible to devise design changes which try to address the problem of *global loss minimization*. Local and global (i.e., relating to the entire machine or process) entropy values are not difficult to compute, but their correct calculation requires very accurate velocity- and temperature fields, so that, with some notable exceptions [2,3,6,9,13,14] losses have not been associated to their corresponding entropy generation rates until relatively recently.

In particular, [14] reports the results of an entropy calculation on a 3-D gas turbine blade: though similar in principle to that approach, our calculation is more accurate, in that it is based on the local values for $\dot{S}$ [1] and does not require the solution of an indipendent set of equation.

The analysis is performed on a two-dimensional cascade at medium Reynolds number Re_{chord}=22500, sub-sonic Mach number Ma_{inlet}=0.27, and steady state. The full Navier-Stokes equations of motion for the turbulent flow of a viscous, compressible fluid, together with the energy equation (in its static-enthalpy formulation), are solved via a standard finite elements code with a k-ε closure, to obtain complete velocity- and

temperature fields, which are then used to compute the entropy generation rates corresponding to the viscous- $\dot{s}_v$ and thermal $\dot{s}_t$ dissipation.

Specifically, the dependance of these entropic losses on the angle of attack for a turbine first-row rotor has been investigated: the reference configuration being a blade at nominal angle α_0=-0.4°, and with cooling air discharge from the tip only (to avoid introducing an additional type of losses due to the mixing of the cooling air ejected from the cooling holes with the mainstream gas).

It is shown that the *thermo-fluiddynamic performance* of each configuration can be assessed at two levels:

i- a *local* level, by examining the local entropy generation rates at each point of the computational domain: these rates tend to increase in the immediate surroundings of the stagnation point, and their maximum is shifted along the leading edge by a change in angle of attack;

ii- a *global level*, by considering the integral value (over the whole of the domain) of the entropy generation rates, vz. of their ratio $\dot{s}_v/\dot{s}_t$, which can be expressed in terms of a dimensionless *dissipation number* [1,13], named after Bejan who first gave a comprehensive treatment of a similar problem [1]. Since the blade cannot be designed to perform equally well under different angles of attack, its overall losses, and correspondigly its global entropy generation rate, will in general increase for off-design conditions.

A standard geometry [7] has been considered, and a commercial finite-element package (FIDAP, by FDI Inc.) has been slightly modified to allow for the calculation of the *local* values of the entropy generation rates, the thermal- and viscous portions of which have been computed separately.

The results at design point are shown to agree well with the available cascade performance data. Those at off-design conditions show that the viscous- and thermal losses are in a nonlinear (and partly unexpected) functional dependance on the angle of attack.

The so-called entropy loss coefficient has been computed [6,9]:

$$\zeta = \frac{T_0 \Delta s}{h_{1s} - h_{2i}} \qquad 1)$$

where T_0 is the reference ambient temperature, Δs is the *total local* entropy generation rate (sum of the viscous- and thermal components), and h_{1s} and h_{2i} are the stagnation enthalpy upstream of the rotor and the ideal exit enthalpy respectively

The results are shown under the form of c_p - and ζ graphs, are representative of realistic situations which could arise in actual gas turbine rotors, when the volume flowrate at the exit of the first nozzle is varied, and the meridional component of the absolute velocity correspondingly varies.

2- VISCOUS AND THERMAL ENTROPY GENERATION IN A CASCADE

Consider the expansion in the first stage of a gas turbine (fig. 2). For a fixed expansion ratio (i.e., for a fixed p_2, the temperature of the gas at the stage exit, T_2, will be *higher* than the corresponding isentropic value T_{2i}: the difference is due to a series of dissipative effects, which result in an effective loss of "work" (in a more precise sense, of exergy [11]), and in a degradation of the thermodynamical quality of the fluid. Both of these effects are expressed by the "lost work" theorem of Guy-Stodola:

$$w_{lost} = T_0 \Delta s$$

Current engineering practice, however, circumvents the exact calculation of the Δs, and recommends the use of *loss coefficients* to take into account the various mechanisms which represent departures from the ideal case (profile loss, secondary losses, tip-leakage losses): these coefficients are predicted by semi-empirical

correlations [6,7] and, once they have been used to compute w_{lost}, the corresponding entropy increase can be derived from 1) and the expansion line can be properly traced.

The most widely used among these coefficients is the *stagnation pressure loss coefficient*, Y, defined as:

$$Y = \frac{p_{01} - p_{02}}{p_{02} - p_2}$$

which is easily measured in cascade tests. Another useful coefficient is the *enthalpy loss coefficient*, ΔH, which is directly linked to the stage efficiency:

$$\Delta H = \frac{h_2 - h_{2i}}{h_{2s} - h_2}$$

As pointed out in [6] though, the only definition which is of interest in turbomachinery design and applications is the so-called *stage isentropic efficiency*, defined as the ratio of the actual- to the isentropic work:

$$\eta_s = \frac{h_1 - h_2}{h_1 - h_{2i}}$$

The *global* measure of the performance deterioration, i.e., of the physical reason which causes the actual work to be lower than the work that would be expected if the expansion was isentropic, is of course the Guy-Stodola lost work and, in end effect, *the entropy generation* of the process. So, it appears that, *entropy generation is the only consistent measure of the lost work due to irreversibilities*. Recently, several Authors [2,3,6,8,9,11,13] have employed the entropy generation concept as a measure of the irreversible losses in gas turbine components, and the results are very promising. Specifically, the use of entropy generation rates to quantitatively measure the work lost in irreversibilities has the following advantages over "loss coefficients" methods (the following list being taken from [9]):

1) specific entropy generation rates do not depend on the frame of reference (rotating or fixed);

2) neither do they depend on mass or volume flowrate (they scale in dynamic similitude);

3) they can be easily split into their viscous- and thermal contributions;

4) they enjoy the additive property: they can be computed separately for each single stage and then summed up to obtain the overall machine irreversibility; furthermore, they can be computed for *one* blade passage and -in the assumption of flow periodicity- multiplied by the number of passages in the cascade;

5) they are implicitly dependent on the temperature level at which irreversibilities take place, i.e., they give a *weighed* loss assessment.

6) they can be used to define a more rational measure of performance, the *entropy loss coefficient*:

$$\zeta = \frac{T_0 \Delta s}{h_{1s} - h_{2i}}$$

The value of the entropy generation rate can be computed from a *global* point of view, using the perfect gas approximation:

$$s_2 - s_1 = c_p \ln\left(\frac{T_2}{T_1}\right) - R \ln\left(\frac{p_2}{p_1}\right)$$

and:

$$\dot{s}_{1-2} = \dot{m}\left(s_2 - s_1\right)$$

or can be computed in a *local* perspective, considering the thermal and viscous contributions to the overall dissipation [11]:

$$\dot{S}_{1-2} = \int_V \left(\frac{\mu\Phi}{T} + \frac{k(\nabla T)^2}{T^2} \right) dV$$

In the right-hand side of equation 8), the first term in the integrand represents the irreversible entropy production rate due to local shear (ϕ being the so-called dissipation function which includes in this case the contribution of the turbulent stresses as well), while the second term represents the irreversible entropy production due to local thermal imbalances: here, these two contributions will be handled separately, and indicated by $\dot{S}_v$ *viscous entropy generation rate* and $\dot{S}_t$ *thermal entropy generation rate* respectively.

The procedure proposed in this work can now be described on the basis of the above remarks. For a given cascade configuration, if a complete quantitative description of the velocity- and temperature fields is available, one can compute $\dot{S}_v$ and $\dot{S}_t$ $\dot{S}_t$ *locally, i.e., in every point of the flowfield*; their integral over the entire flow domain (equation 8) gives then a value which is numerically identical to the $\dot{S}_{1-2}$ obtained by equation 7), and is therefore a measure of the work lost in viscous- and thermal irreversibilities in the flow; notice however that the two contributions in equation 8) can be computed separately, while this would not be possible if one used equation 7). Now, if the cascade configuration is modified, for instance by varying the inlet velocity vector, the same calculation can be repeated, and the new values of $\dot{S}_v$ and $\dot{S}_t$, as well as their integral over the entire flow domain, will *allow a direct comparison of the relative performance of the off-design configuration with respect to the original one*, and, what is perhaps even more important, will *show the map of the viscous-and thermal irreversibility distribution in the flow domain*. The information thus gathered is of significance to the designer who can use it to:

a) choose the configuration which produces the lower total irreversibility (lower entropy generation rate, eqtn. 8);

b) determine -by inspection- where design changes might be desirable to reduce irreversible losses under the applicable design constraints.

c) determine -also by inspection- which design changes might be desirable to reduce irreversible losses at off-design conditions.

The following Sections describe an application of this procedure to a first-stage air-cooled rotor of a gas turbine.

3- AN AIR-COOLED, 2-D ROTOR BLADE AT DESIGN AND OFF-DESIGN CONDITIONS

Consider a two-dimensional section of a gas turbine first-row rotor blade (fig. 3): this is a highly loaded gas turbine blade for which extensive experimental data have been provided for high-Mach flow at ambient temperature [7]. For the purpose of the present study, the profile can be taken as being representative of the radial mid-section of a generic gas turbine vane, internally cooled by a radial flow of air (perpendicular to the plane of the drawing in fig. 3) through three separate internal slots. In the configuration analyzed in this study, the cooling air is assumed to be discharged from the vane tip.

3.1- Cascade data

The relevant geometric parameters of the blading, together with the flow characteristics, are briefly reviewed herebelow.

a) design conditions ("A" in fig. 4)

- chord length L_c = 0.05 m;

- inlet velocity $U_{ref} = W_1$ = 215 m/s;

- inlet gas temperature T_{gas} = 1300 K;

- ambient reference temperature T_0 = 300 K;

- angle of attack α = -0.4°;

b) off-design configurations with increased meridional velocity component ("B" and "C" in fig. 4)

- all parameters as above, except:

- α, which assumes the values -4.4° and -8.4°;

c) off-design configurations with decreased meridional velocity component ("C" and "D" in fig. 4)

- all parameters as above, except:

- α, which assumes the values 3.6° and 7.6°;

The values assumed for the air- and material properties, as well as the dimensionless characteristic flow parameters, are shown in Tables 1 and 2.

3.2- Boundary conditions

The boundary conditions were the same for all four configurations, the only difference being of course the flow direction at the inlet boundary.

- Inlet velocity: fully turbulent, symmetric profile with $W_\infty = W_1$ = 215 m/s

(Notice that this velocity is measured in the reference system moving with the blade, and is therefore a *relative* velocity: the proper velocity triangles are shown in fig. 4);

- Inlet temperature: plug profile, with T_∞ = 1300 K;

- Inlet turbulent quantities: $k_\infty = 0.03\ V_1^2$;

- $\varepsilon_{infty} = 5\ 10^{-6} V_1^3 / L_c$;

- Blade inner wall temperature: T_{inside} = 1118 K;

- Outflow conditions: $\frac{\partial T}{\partial n} = \frac{\partial W}{\partial n} = \frac{\partial k}{\partial n} = \frac{\partial \varepsilon}{\partial n} = 0$

- Notice that no esplicit pressure b.c.'s are needed.

3.3- The numerical procedure

The computational domain and the numerical mesh are shown in fig. 5: since circumferential periodicity is assumed, only a portion of the 2-D cascade (a "cell" containing one blade) is actually computed. The final mesh, consisting of 16718 gridpoints, arranged on 16384 isoparametric quadrilateral four-nodes elements, is similar to the one used in previous work by the same Authors [9,10].

The full Navier-Stokes equations with the addition of the energy equation and of the ideal gas state relation were solved in a rotating frame of reference: notice that the entire procedure was made dimensionless to achieve larger generality; the scaling quantities are listed in Table 2.

Turbulence has been modeled with a two-equations, k-ε model, which requires wall functions to represent the law-of-the-wall profiles for velocity and temperature; the turbulent kinetic energy k and the turbulent dissipation ε are approximated by scaling laws in the wall layer, and their values are then matched to the free-stream calculations.

In the wall layer, k is taken to scale as the square of the distance from the wall, while ε is proportional to k:

$$k = c_k y^{+2} V^2$$

$$\varepsilon = \frac{\left(c_\mu^{0.5} k\right)^{3/2}}{\kappa y^+} \left[1 + \ln\left(\frac{y}{y^+}\right)\right] \frac{V_1^3}{L_c}$$

The code used for the numerical simulation is FIDAP, a commercial F.E. package, which was supplemented with all the additional numerics required for the calculation of the entropy generation rates. FIDAP provides several solution strategies for 2-D and 3-D viscous problems: we chose the so-called "segregated" approach, in which each variable (u, v, p, T, k, ε) is solved for independently, and its solution at the i-th iteration is substituted in the remaining equations at the (i+1)-th iteration. The specific dimensionless form of the equations and details of the solution procedure are described in Appendix I.

Finer meshes are tested (21500, 20816, 18616 nodes each), but it was found that the results obtained with a coarser mesh (16718 nodes) were equivalent, in terms of accuracy, to those obtained with a finer mesh.

Convergence was measured by two parameters: the relative error and the residual error, respectively defined (for a generic variable ϕ) as:

$$e_r = \frac{\phi_i - \phi_{i-1}}{\phi_i}$$

$$r_r = \frac{\|R_i\| - \|R_{i-1}\|}{\|R_i\|}$$

A solution was considered to have converged when $e_r \le 1\%$ and either $r_r \le 1\%$ or $(r_{r_i} - r_{r_{i-1}}) \le 5\%$. The initial flow conditions were taken in all four cases from a laminar converged solution (Re = 400): typically, full convergence was achieved after 200 ÷ 250 iterations.

The flowfield resulting from a converged solution was then used to compute the values of the entropy generation rates, which in the 2-D formulation adopted here are given by the following expressions:

$$\dot{s}_v = \frac{2\mu}{T}\left\{\left(\frac{\partial u}{\partial x}\right)^2 + \left(\frac{\partial v}{\partial y}\right)^2 + \frac{1}{2}\left(\frac{\partial u}{\partial y} + \frac{\partial v}{\partial x}\right)^2\right\}$$

$$\dot{s}_t = \frac{k_{air}}{T^2}\left\{\left(\frac{\partial T}{\partial x}\right)^2 + \left(\frac{\partial T}{\partial y}\right)^2\right\}$$

The procedure used for numerically computing the *elemental* values of $\dot{s}_v$ and $\dot{s}_t$ is also described in detail in Appendix 1.

The values thus obtained for $\dot{s}_v$ and $\dot{s}_t$ are considered to be *element averages*, and are ideally assigned to the centroid of each element: this produces a map of the entropy generation rates over the computational domain, represented by two discrete functions (whose values are known at the centroid of each element), $S_v(x,y)$ and $S_t(x,y)$. The total entropy generation rates over the entire flow domain can be obtained by numerically integrating these functions, which can be easily done by weighing the nodal values by the proper element "volumes" (in 2-D, areas) and summing over all fluid (and, where applicable, solid) elements. It has to be remarked that the numerical dissipation (which is introduced in the computations by the so-called upwinding factor) is of order O(d/4), where d is the rms value of the elements diagonals. Since $d \cong 0.021 L_{ref}$, the ratio of the numerical to the actual dissipation is approxmately 0.0053

4- RESULTS AND DISCUSSION

The details of the numerical solution are shown in figs. 6 ÷ 8 (not all cases are shown here: the general large-scale features of the flowfields are *similar* for different angles of incidence, and the differences are detectable in the detailed maps of $\dot{s}_v$ and $\dot{s}_t$ given below). The velocity and temperature profiles are in general agreement with the flow patterns that one would expect in such a cascade: notice that the results presented in [7] are for a fully compressible situation (at room temperature; Ma_{inlet} = 0.5, Ma_{outlet} = 1.2), while the solution obtained here is for much lower Ma_{in} (0.27), so that the overall flow can be regarded as almost-incompressible, but for a much higher inlet temperature. Furthermore, [7] contains no explicit discussion of off-design performance. So, the only conclusion that can be drawn from these flowfields is that the simulation reproduces the *general features* of the flow as expected. The same remarks apply to some of the cascade performance parameters which can be calculated from the thermo-fluiddynamic fields: the pressure coefficient (fig. 9) and the blade temperature distribution (fig. 8) both show some interesting features which are discussed elsewhere [11].

What is of interest here is to examine in detail the entropy production rates and their distribution, to assess the merit of the proposed procedure, which (see Sections 1 and 2 above) predicts the possibility of relating the *performance* of a cascade to its *total entropy production*. Considering the maps of the viscous- and thermal entropy generation rates (for the design case) shown in fig. 11 and 12, and their global (integral) values shown in fig. 13, the following conclusions can be drawn:

1) both $\dot{s}_v$ and $\dot{s}_t$ are almost entirely produced in the boundary layer around the blade (Figures 11 & 12), due to the high local gradients at the wall. This agrees with the results discussed in [14], if one considers that 3-D effects (end-wall, tip leakage, etc.) are negated by our 2-D assumption. A variation of α induces a modification of the *local* characteristics of the boundary layer in the vicinity of the stagnation point, and the distribution of the viscous entropy generation rate changes accordingly: this result was to be expected. One would also expect that a departure from the design conditions brings about an increase of the irreversible losses, i.e., that the value of the integral of $\dot{s}_v$ over the entire domain increases with $\Delta\alpha$ (where $\Delta\alpha = \alpha_{design} - \alpha_{off\text{-}design}$), *no*

matter whether the sign of $\Delta\alpha$ *is positive or negative*. Figure 13 shows that the increase is almost quadratic (one would expect indeed a quadratic dependence of the viscous losses with α).

2) Blade performance, measured by the irreversibility coefficient ζ, remains almost constant for small variations of α around its design value, but decreases substantially for angles of attack far from it. This means that the blade leading edge can accomodate small variations of flowrate without severe performance deterioration.

3) The cooling effectiveness of the given configuration is only slightly affected by a variation of the angle of attack (determined on the basis of the blade surface heat flux profiles, fig. 10): but the thermal entropy production varies of a non-negligible amount, as shown by its global value (integral of s_t over the entire domain, fig. 13). The conclusion is that the temperature distribution *around* the blade does contribute significantly to the overall irreversibility of the expansion process.

4) The local Bejan number, $Be = \dfrac{\dot{s}_t}{\dot{s}_v - \dot{s}_t}$, which gives an indication of the relative importance of the two causes of flow irreversibility, attains (fig. 15, case A) a value of about 0.5 in the vicinity of the wall, where the two contributions $\dot{s}_v$ and $\dot{s}_t$ are of the same order of magnitude, reaches a peak value of about .95 in the so-called "inviscid" flow region, where $\dot{s}_v$ is negligible and s_t is produced by turbulent convective mixing, and it is almost zero (≈ 0.05) upstream of the vane and in the "isothermal core" which constitutes the central portion of the interblade space. Near stagnation point, Be is about $0.4 \div 0.6$, showing that the two irreversibilities are of the same magnitude. These values are not substantially modified by a change in the direction of the incoming flow velocity, and one may conclude that Be is not a proper parameter to use in this analysis. Indeed, the value of the global Bejan number (i.e., of the integral of Be over the entire flow domain), shows very little variation with α, confirming that the ratio of the two irreversible entropy production rates does not change with a variation of the flowrate coefficient ϕ, at least within the range covered by the present investigation.

These conclusions -as remarked in [9]- ought to be viewed with caution, for two reasons: first, the simulation being at steady-state, the details of the flow are obviously valid only as "statistical averages", and the time-dependent details of the solution are entirely neglected; second, since the turbulence has been modeled by a k-ε closure, the behaviour of the turbulent quantities in the vicinity of the wall has been imposed *a priori* by the choice of model parameters, and, since most of $\dot{s}_v$ and s_t are produced in the sub- and inner layers, the results might be strongly model-dependent.

These objections could be addressed by performing a time-dependent simulation in unsteady flow conditions and using a different turbulence modeling, but then it might become more important to take three-dimensional or shock-related effects into account than to change the near-wall model. These remain open issues, and ought to be investigated in the future.

5- CONCLUSIONS

A procedure which links the losses in a cascade to the irreversible entropy production, described in [9,10], is applied in this paper to the assessment of off-design performance of a 2-D rotor cascade.

The total entropy generation rate $\dot{S}_{tot}$ is a convenient performance parameter to use in practice, because it offers several advantages over other efficiency parameters:

1) $\dot{S}_{tot}$ can be computed numerically from known flowfields (where local values for both velocity and temperature are available);

2) it can be readily linked to the *real* efficiency of the machine of which the cascade is a component through - for example- the "entropy loss" coefficient [6] or the dimensionless Bejan number [11], or the Guy-Stodola lost work;

3) it can be conveniently split into its viscous- and thermal contributions, thus allowing better insight in the flow phenomena;

4) it contains information at two physical levels: at a *local* level, it shows how and where irreversibilities are present, and to what extent they can be removed by design changes; at a *global* -or integral- level, it gives a measure of the "degree of irreversibility" of the flow process in the cascade, which enables a designer to assess the relative performance of different configurations.

The procedure has been applied to a 2-D model of a first-row rotor vane of a gas turbine, for which the massflow coefficient ϕ has been varied, producing a range of different angles of attack. The results show that it is indeed possible to assess the off-design performance of a cascade looking at its irreversible losses, and that the two effects (viscous and thermal) can be easily separated.

These results confirm those already described in [9,10], and the conclusions which were stated in those previous studies can be repeated here:

i- the procedure (which was applied to a stator vane in [9]) is indeed feasible and shows potential for being applied to real industrial (3-D) configuration studies;

ii- there are areas which require further investigation. In particular, the turbulence model (especially the wall functions) is likely to affect the absolute numerical value of the computed entropy generation rates; further, unsteady effects can change the picture: endwall and wake losses, tip leakage effects, and interactions with upstream flow disturbances can change the relative importance of the two effects $\dot{s}_v$ and $\dot{s}_t$;

iii- in general, the procedure is only as good as the underlying numerical data: if -however- experimental data about the flowfields are known, the calculation of $\dot{s}_v$ and $\dot{s}_t$ is straightforward.

APPENDIX 1
THE GOVERNING EQUATIONS AND THE NUMERICAL SOLUTION PROCEDURE

The governing equations are the Navier-Stokes equations in their cartesian formulation, the continuity- and the energy equation, and the ideal gas state relation; the problem is 2-D, steady, and with constant fluid properties. The dimensionless form of the equations read as follows (summation convention applies):

$$u_j \frac{\partial u_i}{\partial y_j} = \frac{\partial p}{\partial x_i} + \frac{1}{Re}\left(\frac{\partial^2 u_i}{\partial x_i \partial y_j}\right) \qquad A.1)$$

$$\frac{\partial u_i}{\partial x_i} = 0 \qquad A.2)$$

$$u_j \frac{\partial T}{\partial x_j} = D \frac{\partial^2 u_i}{\partial x_i \partial x_j} \qquad A.3)$$

The code used for the simulation (FIDAP, trademark of FDI Inc.) has several built-in turbulence models: a modified mixing lenght model, and a k-ε two equation model. The k-ε has been employed here, and the equations are of the form:

$$u_j \frac{\partial k}{\partial x_j} = \frac{1}{\mu_t \, \mathrm{Re}} \frac{\partial^2 k}{\partial x_i \partial x_j} + f_1(k, \varepsilon, \mu_t) \qquad \text{A.4)}$$

$$u_j \frac{\partial \varepsilon}{\partial x_j} = \frac{1}{\mu_t \, \mathrm{Re}} \frac{\partial^2 \varepsilon}{\partial x_i \partial x_j} + f_2(k, \varepsilon, \mu_t) \qquad \text{A.5)}$$

$$u_t = f_3(k, \varepsilon) \qquad \text{A.6)}$$

The equations are discretized with a standard finite element procedure, and the solution is obtained by an iterative "segregated" method, which solves for each variable (u, v, T, k, ε) separately, using the values of the other variables known from the previous iteration.

For the initial flowfield, an increment step procedure has been followed: first, a laminar solution (Re = 400) is obtained starting from an isothermal fluid at rest; then, turbulent modeling has been switched on and Re has been increased stepwise (in the present simulation, from 400 to 10000, then 100000 and finally 225000). At each step,, the sollution has been restarted from the converged solution at the lower Re. For a new configuration, the entire process has been repeated from Re = 400.

The entropy generation rates have been computed from the converged flowfield via the following equations (in which indicial notation has been substituted by explicit 2-D notation for the sake of clarity):

$$\dot{s}_v = \left(\frac{\partial u}{\partial x}\right)^2 + \left(\frac{\partial v}{\partial y}\right)^2 + \frac{1}{2}\left(\frac{\partial u}{\partial y} + \frac{\partial v}{\partial x}\right)^2 \qquad \text{A.7)}$$

$$\dot{s}_v = \left(\frac{\partial T}{\partial x}\right)^2 + \left(\frac{\partial T}{\partial y}\right)^2 \qquad \text{A.8)}$$

Notice that these expressions are dimensionless: to compute the dimensional specific entropy generation rates, one must multiply $\dot{s}_v$ and $\dot{s}_t$ respectively by:

$$S_{0v} = \frac{\mu U^2}{L^2 \Delta T} \qquad \text{A.9)}$$

$$S_{0t} = \frac{k_{air}}{L^2} \qquad \text{A.10)}$$

These entropy generation rates are treated as *elemental* variables, i.e., they are assigned to the centroid of the element for which they have been computed. The numerical code, however, as most finite element codes, does not posses derivative continuity at the nodes: therefore, a separate computation was necessary to ensure -at least in an *average* sense- the continuity of the entropy production function. The steps of this procedure are the following:

1) nodal values for the derivatives are computated in the reference system *local* to each element: this can be done analytically once and for all, because the shape functions are known quadratic functions of the local coordinates (r,s);

2) the local value of the derivative is computed by adding the nodal contributions (all elements are four-node quadrilateral):

$$\frac{\partial u}{\partial r} = \sum_{i=1}^{4} \frac{\partial \phi_i}{\partial r} U_i \qquad \text{A11)}$$

$$\frac{\partial u}{\partial s} = \sum_{i=1}^{4} \frac{\partial \phi_i}{\partial s} U_i \qquad \text{A12)}$$

3) the values of the derivative in the *global* reference system is then abtained by moltiplication by the local Jacobian:

$$\frac{\partial u}{\partial x} = \frac{\partial u}{\partial r}\frac{\partial r}{\partial x} + \frac{\partial u}{\partial s}\frac{\partial s}{\partial x} \qquad \text{A13)}$$

and similarly for the other derivatives;

4) in the global reference system, the value of the nodal derivative is obtained by an area-weighed average of the nodal values pertaining to all N elements concurring in the node:

$$\frac{\partial u}{\partial x} = \sum_{i=1}^{N} \frac{\partial u}{\partial x}\frac{A_i}{A_{tot}} \qquad \text{A14)}$$

and similarly for the other derivatives;

5) the values obtained in 4) are then substitued in the formulas for S_v and S_t.

For the wall elements, which have special wall functions to better fit the turbulent logarithmic law of the wall, a slightly different procedure had to be employed:

1)the nodal values at the "top" of the wall element ($y^+ \approx 100$) are taken from the flowfield; values from the wall (where u = v = 0) upwards are calculated on M intermediate points (here, M=5) using the special wall functions: i.e., these intermediate values can be regarded as "exact" (they are as good as the wall function);

2)the derivatives are then calculated *at each intermediate point* by symbolic differentation, resulting in "exact" values (in the sense stated above);

3)the entropy generation rates are computed in each of the 2M points (M for each side of the quadrilateral);

4)the elemental value of the entropy generation rates is then obtained by numerically integrating the 2M intermediate nodal values computed in 3).

- REFERENCES

1- A.Bejan: *Entropy generation through heat and fluid flow*, J.Wiley 1982

2- P.L.Benedetti,E.Sciubba: *Numerical calculation of the local rate of entropy generation in the flow around a heated finned tube*, in ASME AES-3, 1993

3- C.J.Borth,B.M.Argrow: *Evaluatian of entropy productian and numerical entropy change in flowfield solutions*, in ASME-AES-vol.25/HTD-vol.191, 1991

4- R.J.Boyle: *Navier-Stokes analysis of turbine blade heat transfer*, J.of Turbomach., 113, Jul. 1991

5- C.Camci,T.Arts: *An experimental canvective heat transfer investigation around a film-cooled gas turbine blade*, J.of Turbomach., 113, Jul. 1990

6- J.D.Denton: *Loss mechanisms in turbomachines*, J.of Turbomach., 115, Oct. 1993

7- R.Kiock,H.Hoheisel,H.J.Dietrichs,A.T.Holmes: *The baundary-layer behaviar of an advanced gas turbine rotor blades under the influence af simulated film cooing*, ASME-GT-42, 1993

8- R.E.Mayle: *Pressure loss and heat transfer in channels roughened on two opposite walls*, J.of Turbomach., 113, Jan.1991

9- J.Moore,J.G.Moore: *Entropy production rates from viscous flow calculations, Part 1- a turbulent boundary layer*, ASME paper 83-GT-70, 1983

10- G.Natalini,E.Sciubba: *Entropy generation rates in air-coaled gas turbine nozzles: a numerical configuration study*, Proc. IGTI-COGEN-TURBO, 1994

11- G.Natalini,E.Sciubba: *A new criterion far configuration optimization of air-caoled gas turbine blades, based on the minimization of the local entropy production*, in ASME-AES-33, 1994

12- S.Paoletti,F.Rispoli,E.Sciubba: *Calculation of exergetic losses in compact heat exchanger passages*, in ASME AES-10/2, 1989

13- L.Sangiovanni,R.Gusso: *Recent trends in the develapment af gas turbines far combined cycles and cogeneration*, in Proc. ASME-FLOWERS '90, 1990

14- T.J. Sullivan: *Navel aerodynamic loss analisys technique based on CFD predictions of entropy production*, SAE TP 951430, 1995.

15- E.Sciubba: *Numerical calculation of local irreversibilities in compact heat exchangers*, in Proc. NATO-TIBTD Workshop on 2nd Law, Erciyes Univ., Kayseri 1990

16- A.K.Sinha,D.G.Bogard,M.E.Crawford: *Gas turbine film cooling: flowfield due to a secand row of holes*, J.of Turbomach., 113, Jul.1991

17- K.Takeishi,S.Aoki,T.Sato,K.Tsukagoshi: *Film cooling on a gas turbine rotor blade*, J.of Turbomach., 114, Oct.1992

- LIST OF SYMBOLS

α	angle of incidence
$Be = \frac{S_t}{S_v - S_t}$	Bejan number
c_p	specific heat at constant pressure
$\Delta T = T_{gas} - T_{air}$	reference temperature difference
h	enthalpy
k	turbulent kinetic energy

k_{air}	air thermal conductivity
ε	turbulent dissipation
L_c	chord lenght
$\dot{m}$	mass flowrate
μ	air dynamic viscosity
ν	air kinematic viscosity
p	pressure
p_0	stagnation pressure
$\dot{\phi}$	viscous dissipation function
φ	mass flowrate coefficient, $\frac{V_m}{U}$
R	gas constant
$\mathrm{Re} = \frac{U_{ref} L_c}{\nu}$	Reynolds number
s_v	viscous entropy generation rate
s_t	thermal entropy generation rate
T_0	ambient reference temperature
T_c	cooling air temperature
T_{gas}	inlet gas temperature
U	peripheral velocity, ωr
U_{ref}	reference velocity
V	control volume
V_1	absolute inlet velocity
W_1	relative inlet velocity

Table 1
Air and material properties

Air density (kg/m^3)	$\rho_{1300} = 0.2716$ $\rho_{760} = 0.4707$
Air dynamic viscosity (kg/m s)	$\mu_{1300} = 4.88 \cdot 10^{-5}$ $\mu_{760} = 3.5 \cdot 10^{-5}$
Air conductivity (W/m K)	$k_{1300} = 0.0797$ $k_{760} = 0.0541$
Air constant-pressure specific heat (kJ/kg K)	$c_{p1300} = 1.189$ $c_{p760} = 1.087$
Steel conductivity (W/m K)	$k_s = 26$

Table 2
Scaling quantities and dimensionless flow parameters

$L_{ref} = 0.15$ m $U_{ref} = 103$ m/s $T_{ref} = 300$ K	$\dot{s}_{v,ref} = \frac{\mu U^2}{\Delta T L_{ref}^2}$ $\dot{s}_{t,ref} = \frac{k}{L_{ref}^2}$
$\mathrm{Re} = \frac{U_{ref} L_{ref}}{\nu_{1300}} = 86000$ $\mathrm{Pe} = \mathrm{Re}\,\mathrm{Pr} = 60200$	$\mathrm{Pr} = \frac{\nu_{1300} c_{p1300}}{k} = 0.7$
$\Delta T_{ref} = 1000$ K	$\mathrm{Br} = \frac{k \Delta T}{\mu U^2} = 154$

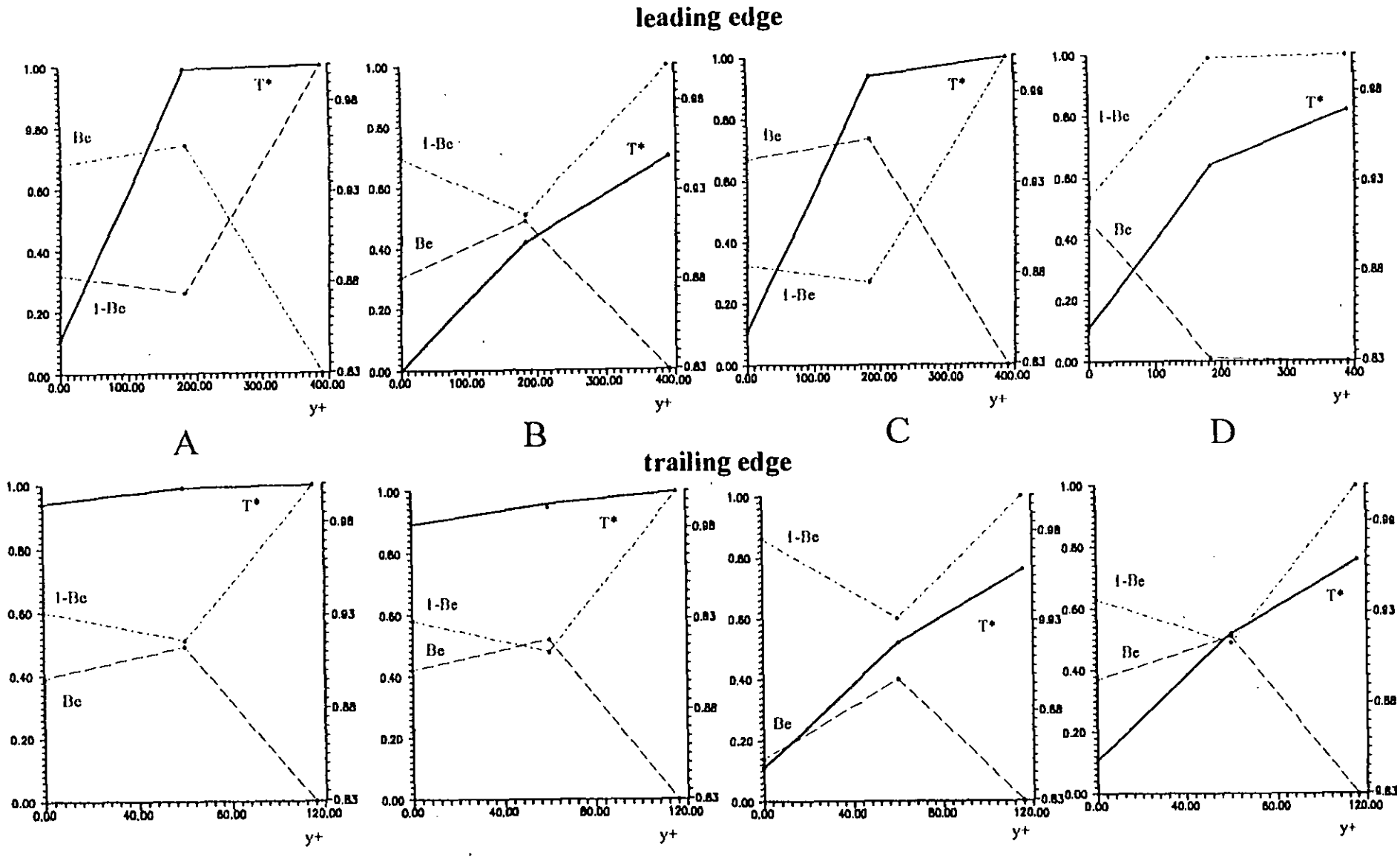

Legenda: A - no film cooling
B - 1 row of cooling holes at the leading edge
C - 1 row of cooling holes at the trailing edge
D - 2 rows of cooling holes

Be ≈ thermal entropy generation rate

1-Be ≈ viscous entropy generation rate

T* = dimensionless temperature

Fig. 15 - Bejan number and entropy generation rates in the wall layers

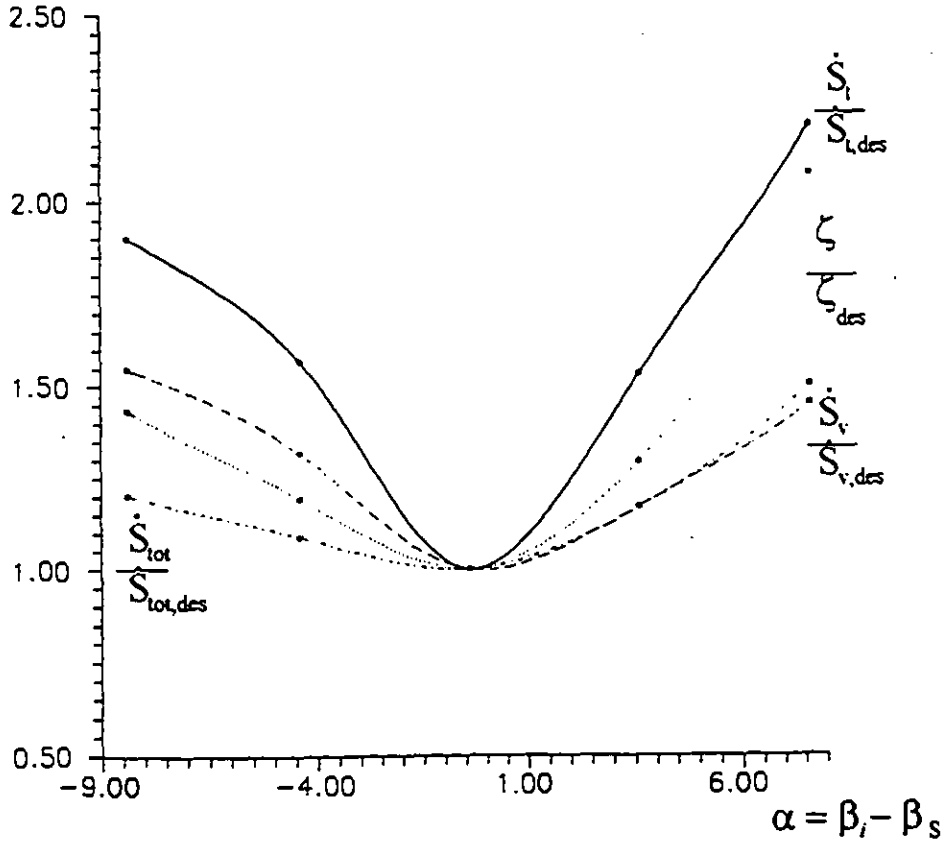

Fig. 13 - $\dot{S}_v$, $\dot{S}_t$, $\dot{S}_{tot}$, and ζ as a function af α

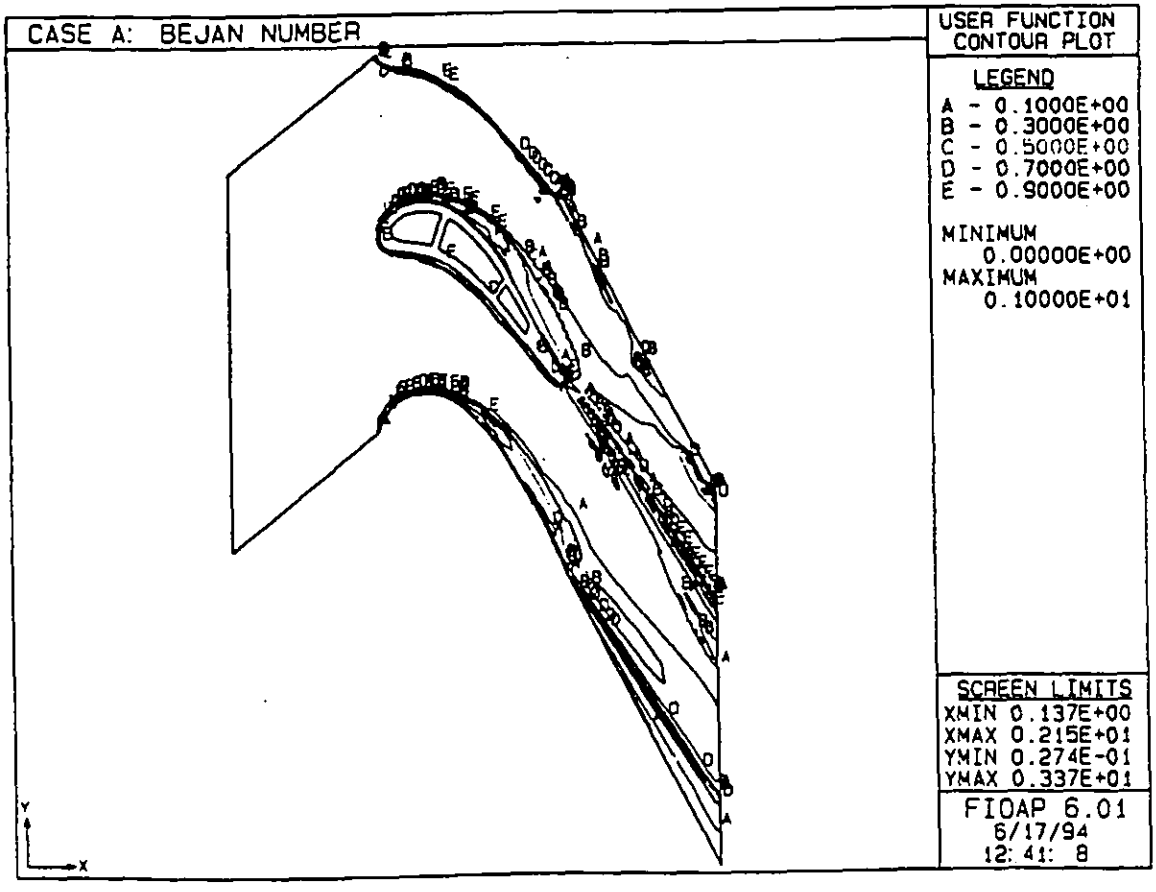

Fig. 14 - Global Bejan number contours at design conditionss

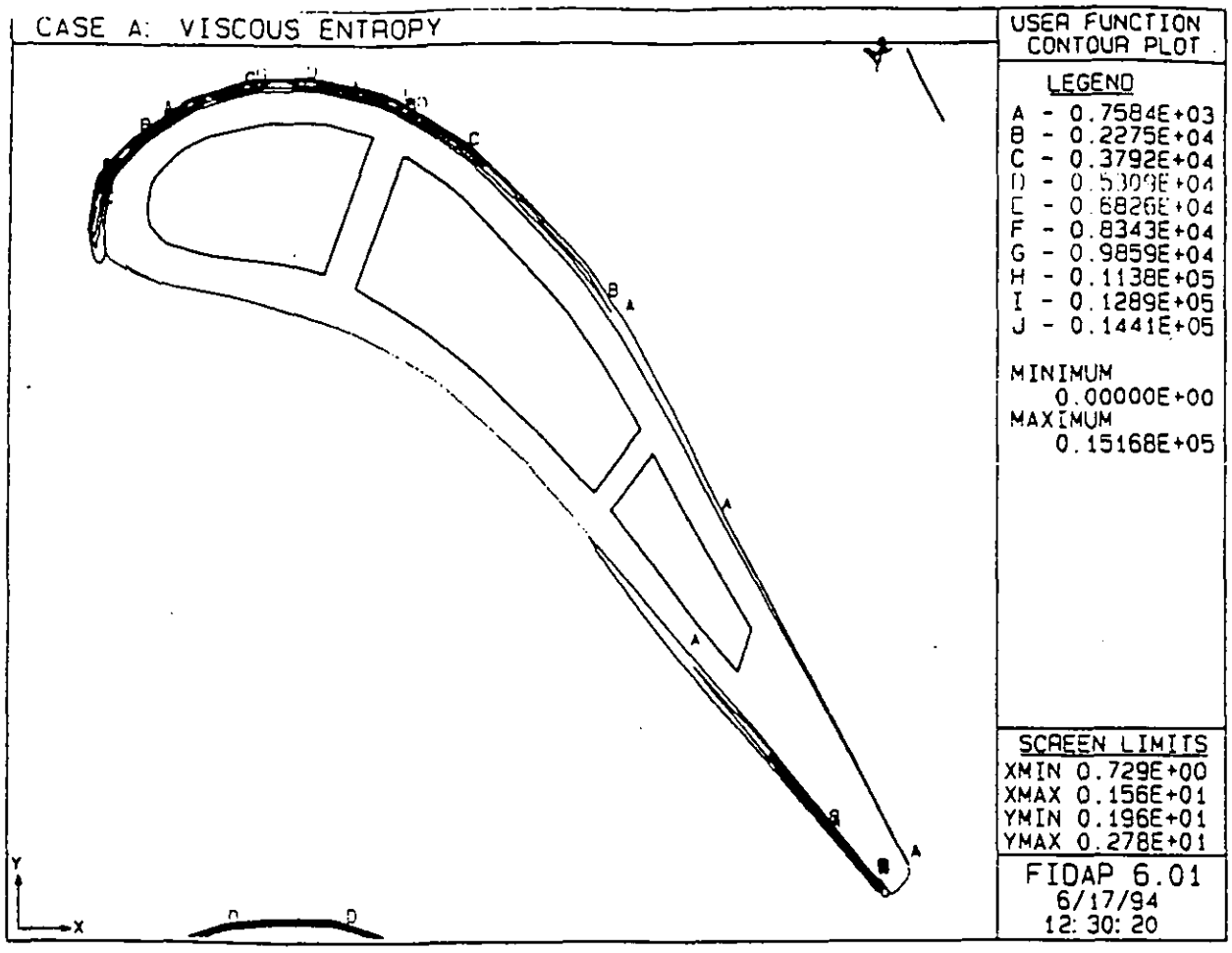

Fig. 11 - Computed viscous entropy generation rates at design conditions

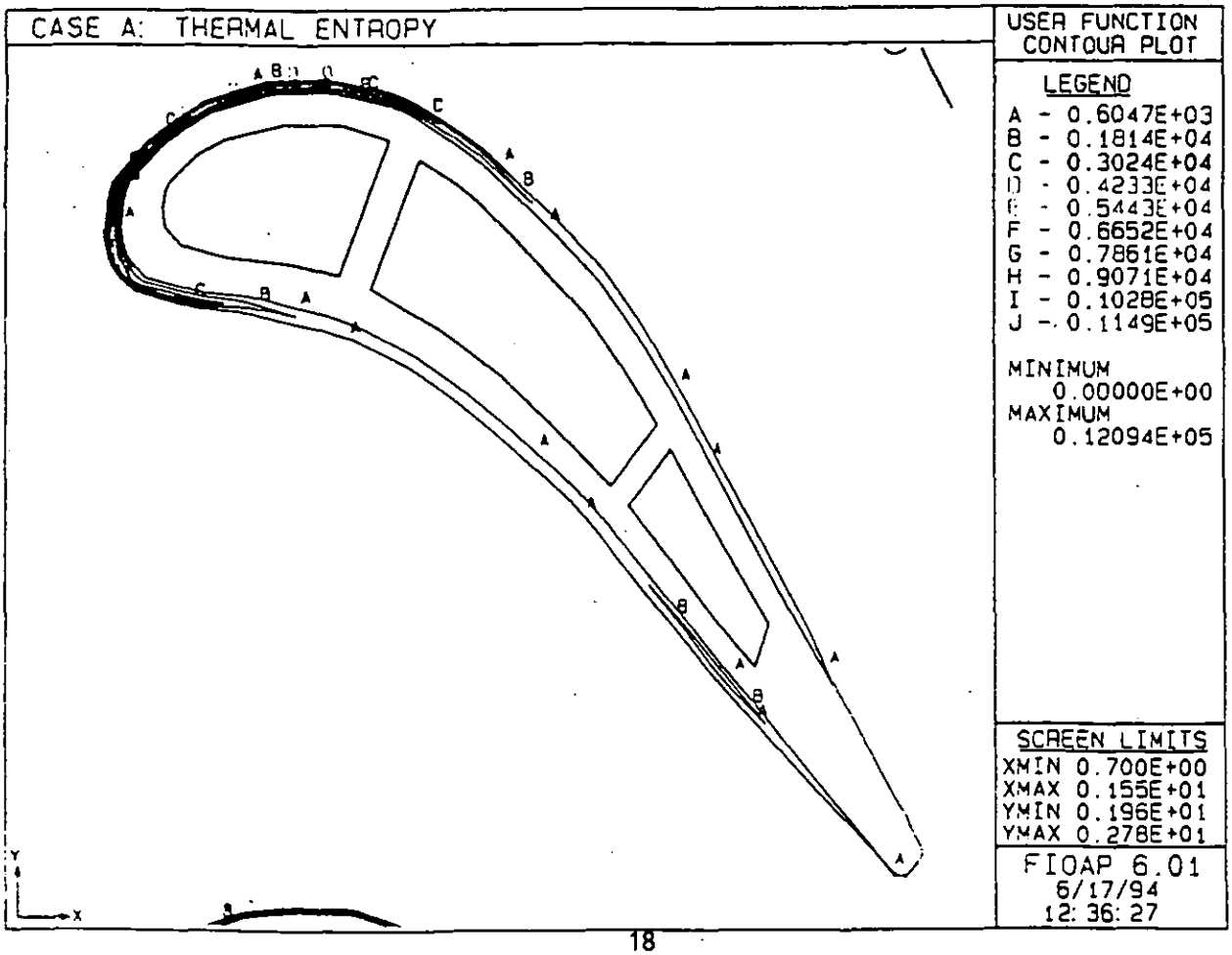

Fig. 12 - Computed thermal entropy generation rates at design conditions

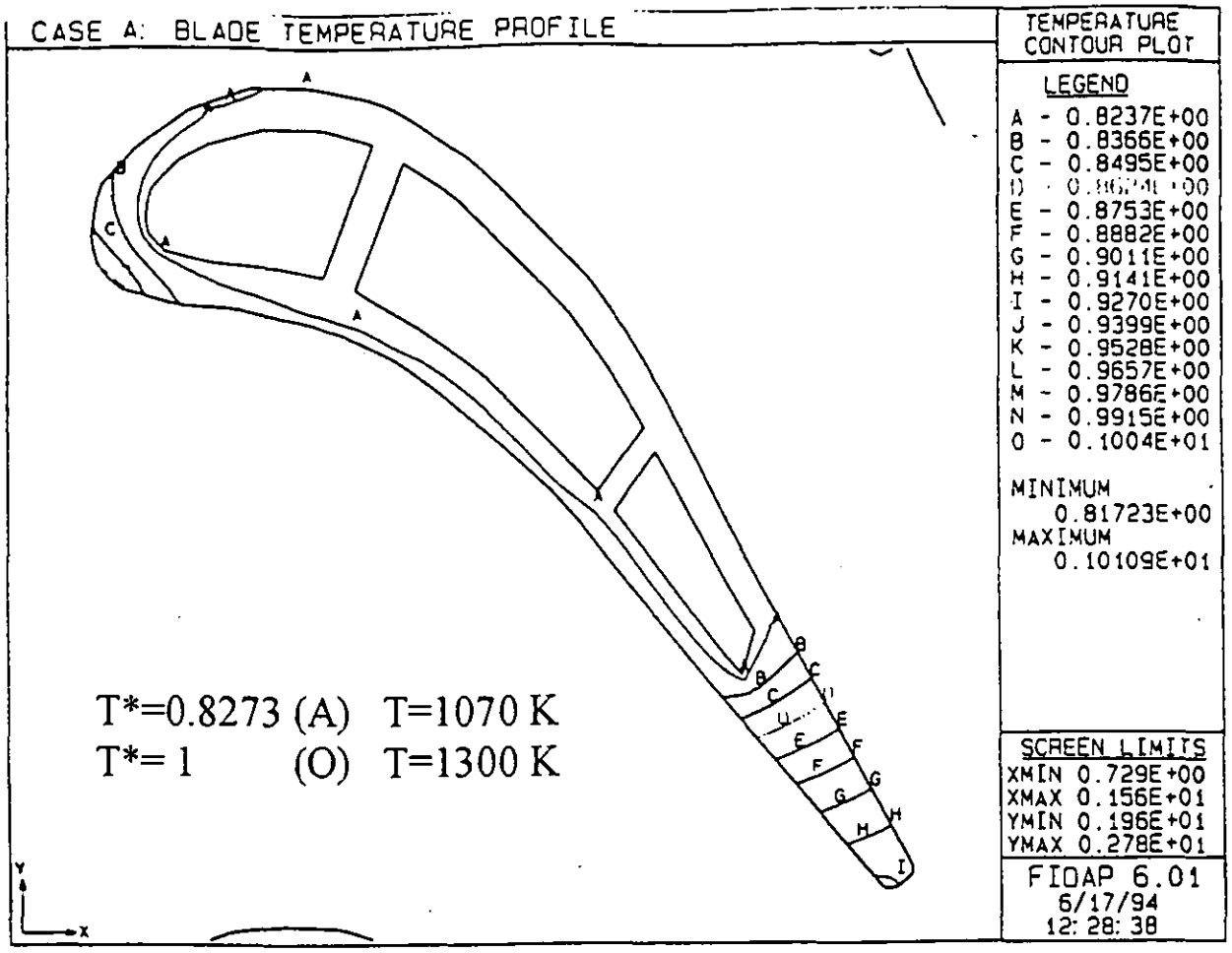

Fig. 8 - Blade temperature contours at design conditions

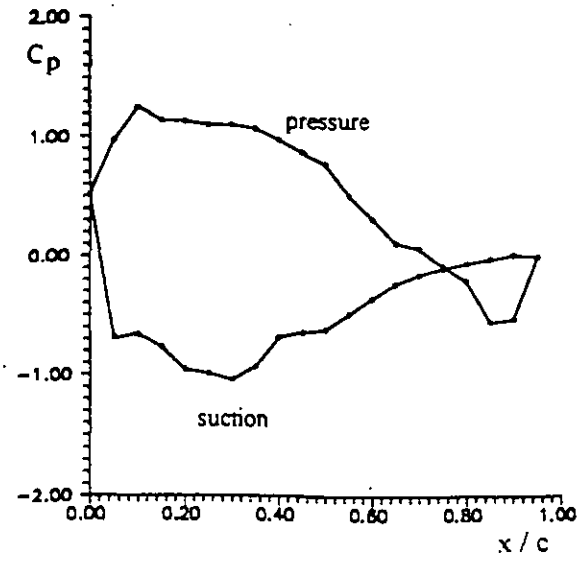

Fig. 9 - Computed pressure coefficient at design conditions

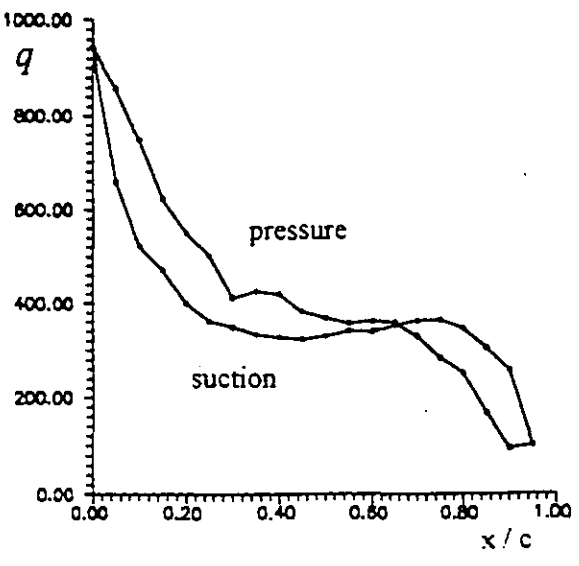

Fig. 10 - Computed blade surface heat flux (W/m^2)

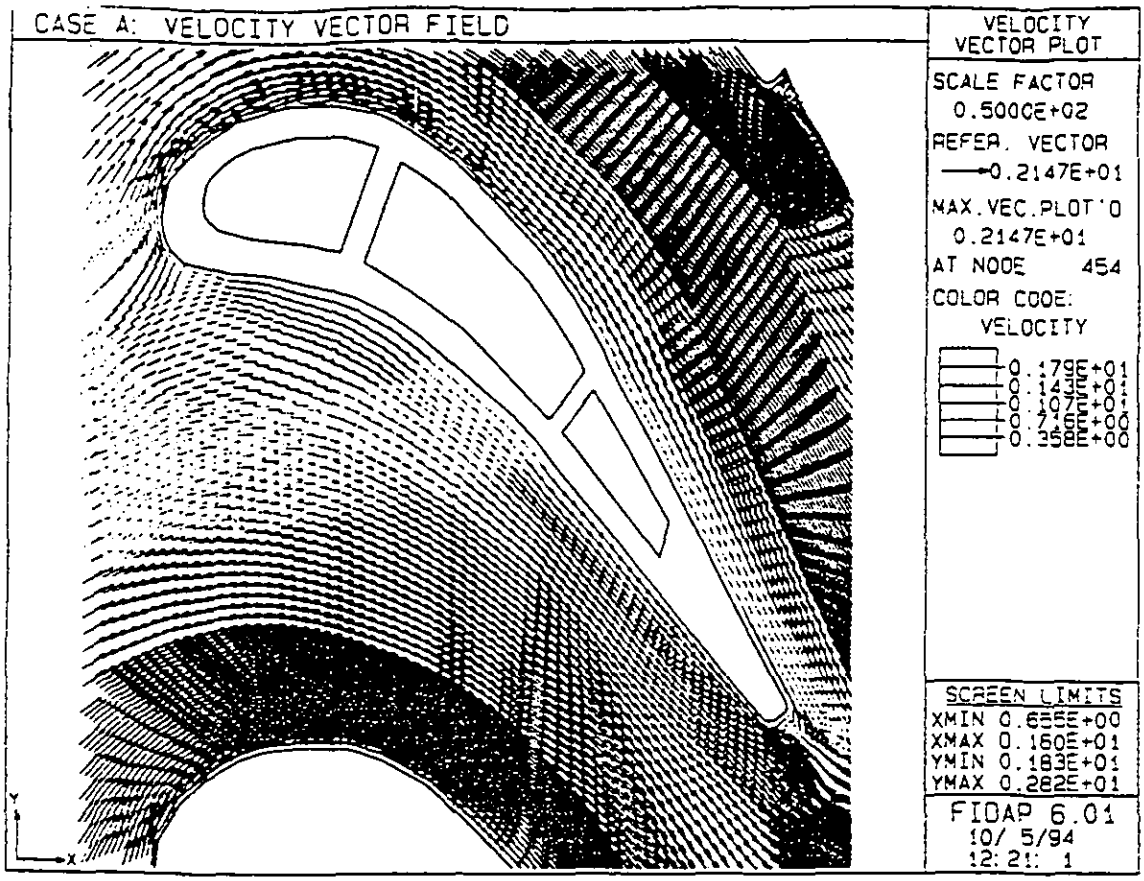

Fig. 6 - The computed velocity vector field at design conditions

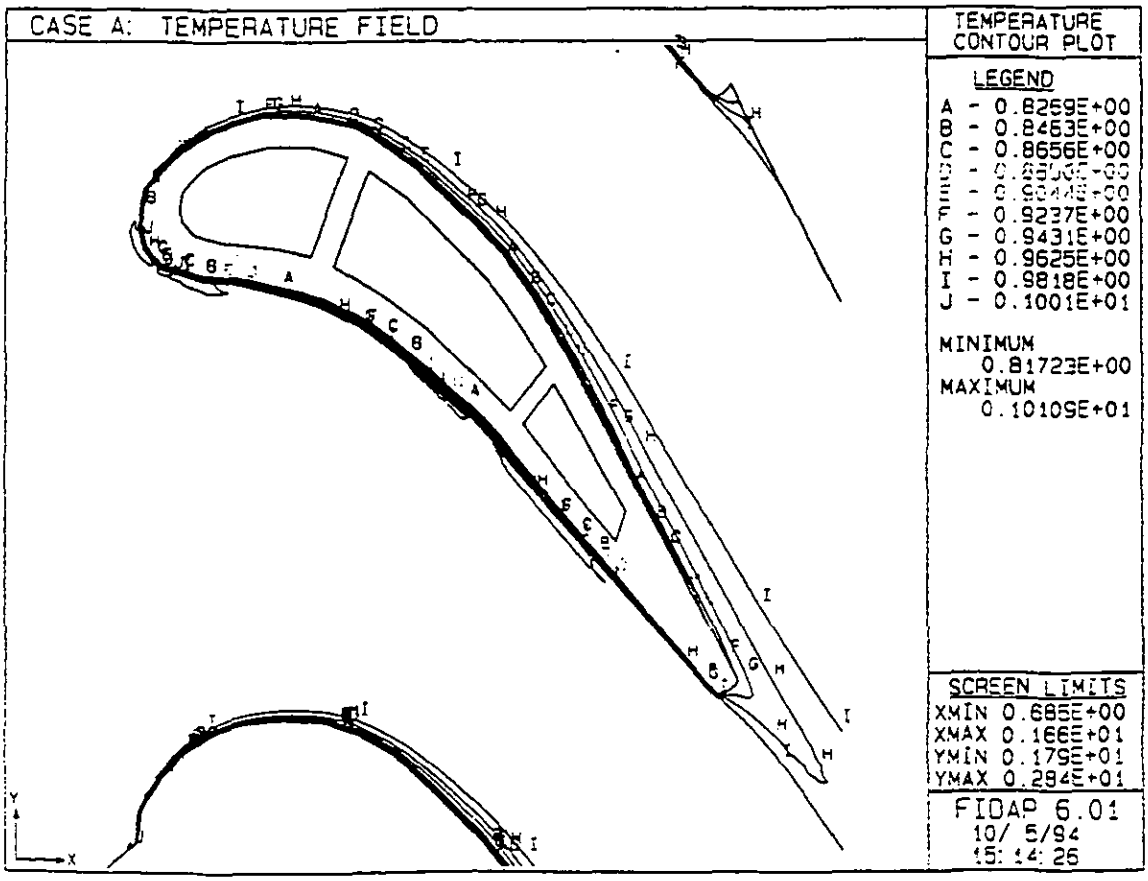

Fig. 7 - The computed temperature field at design conditions

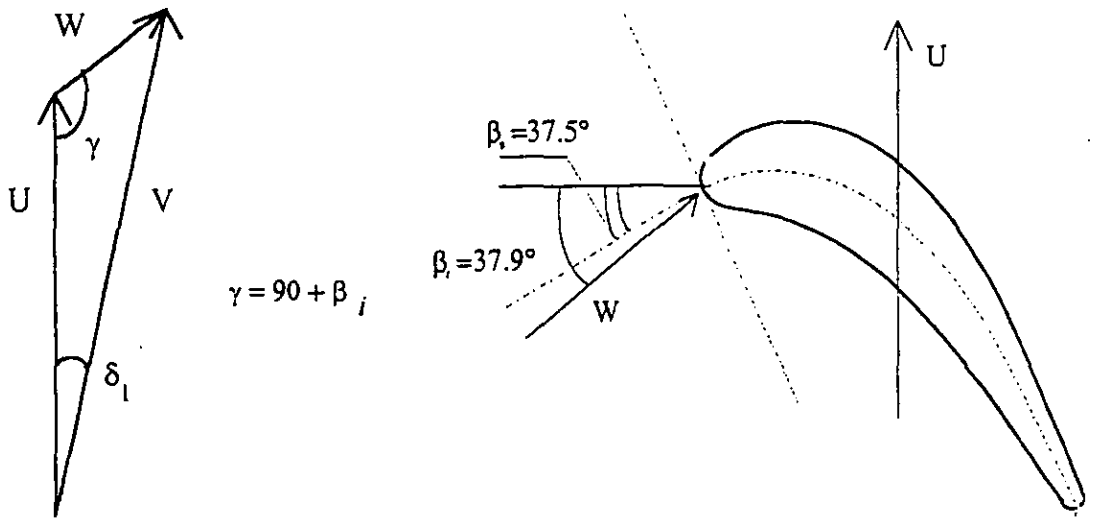

$$V_1 = \left(U^2 + W_1^2 - 2UW_1 \cos\gamma\right)^{1/2}$$

$$V_{1m} = V_1 \operatorname{sen}\delta_1 = W_1 \operatorname{sen}(90 - \beta_i)$$

$$V_{1t} = V_1 \cos\delta_1 = U + W_1 \cos(90 - \beta_i) = U + W \operatorname{sen}\beta_i$$

Fig. 4 a - design conditions

CASE	β_i	α	γ	U (m/s)	V_1 (m/s)	W_1 (m/s)	$\varphi_1 = \frac{V_{1m}}{U}$	$\psi_1 = \frac{V_{1t}}{U}$
A (design)	37.9°	-0.4°	127.9°	400	470	215	0.203	1.158
B	33.9°	-4.4°	123.9°	400	465	215	0.214	1.143
C	29.9°	-8.4°	119.9°	400	460	215	0.223	1.128
D	41.9°	+3.6°	131.9°	400	475	215	0.192	1.172
E	45.9°	+7.6°	135.9°	400	479	215	0.179	1.185

Fig. 4 b - design and off-design parameters

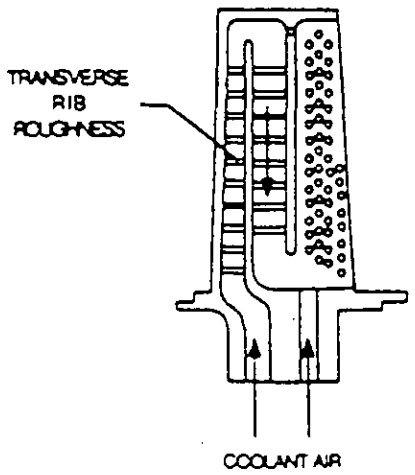

Fig. 1- Typical film cooling arrangement for a gas turbine blade [8]

Fig 2 - Enthalpy-entropy representation of the expansion in the first stage of a gas turbine

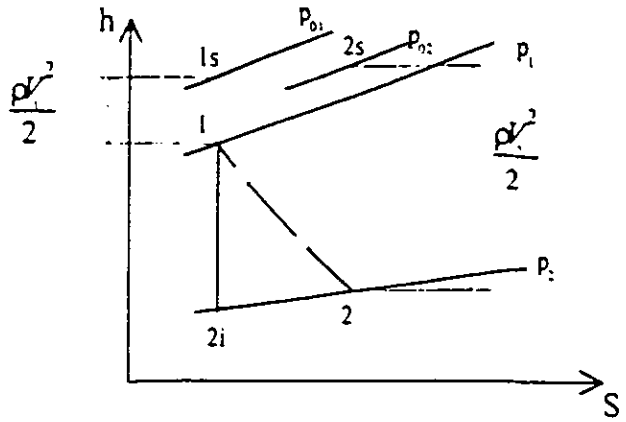

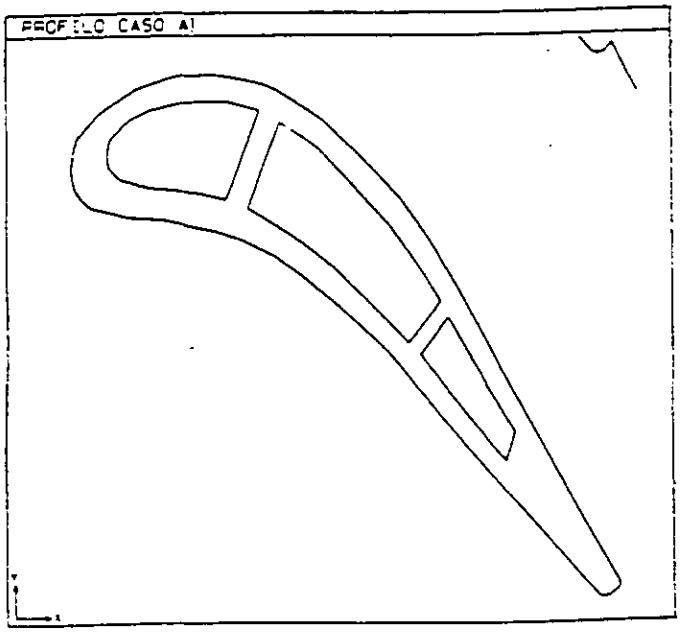

Fig. 3 - Radial mid-section of a representative first-stage nozzle

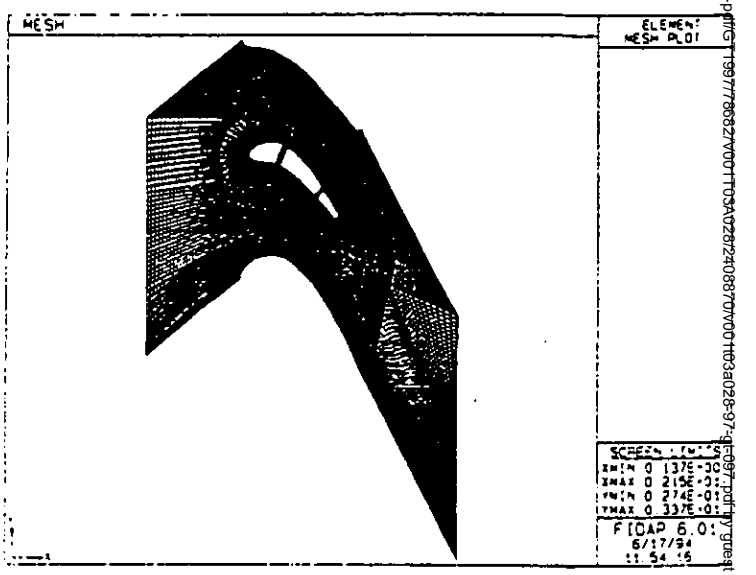

Fig. 5 - The computational domain and the final mesh